Spectroscopic Study and Evaluation of Red-Absorbing Fluorescent Dyes

Volker Buschmann,[†] Kenneth D. Weston,[‡] and Markus Sauer*[,†]

Physikalisch-Chemisches Institut, Universität Heidelberg, Im Neuenheimer Feld 253, 69120 Heidelberg, Germany and Department of Chemistry and Biochemistry, Florida State University, Tallahassee, Florida 32306. Received September 4, 2002; Revised Manuscript Received October 21, 2002

The spectroscopic characteristics (absorption, emission, and fluorescence lifetime) of 13 commercially available red-absorbing fluorescent dyes were studied under a variety of conditions. The dyes included in this study are Alexa647, ATTO655, ATTO680, Bodipy630/650, Cy5, Cy5.5, DiD, DY-630, DY-635, DY-640, DY-650, DY-655, and EVOblue30. The thorough characterization of this class of dyes will facilitate selection of the appropriate red-absorbing fluorescent labels for applications in fluorescence assays. The influences of polarity, viscosity, and the addition of detergent (Tween20) on the spectroscopic properties were investigated, and fluorescence correlation spectroscopy (FCS) was utilized to assess the photophysical properties of the dyes under high excitation conditions. The dyes can be classified into groups based on the results presented. For example, while the fluorescence quantum yield of ATTO655, ATTO680, and EVOblue30 is primarily controlled by the polarity of the surrounding medium, more hydrophobic and structurally flexible dyes of the DY-family are strongly influenced by the viscosity of the medium and the addition of detergents. Covalent binding of the dyes to biotin and subsequent addition of streptavidin results in reversible fluorescence quenching or changes in the relaxation time of other photophysical processes of some dyes, most likely due to interactions with tryptophan residues in the streptavin binding site.

INTRODUCTION

The interest in fluorescent dyes for qualitative and quantitative assays has increased considerably during the last 20 years (*1*−*4*). The sensitivity, simplicity, and selectivity of fluorescence-based techniques make them particular attractive for in vitro and in vivo cellular and molecular biology studies (*5*). There are several major advantages of using fluorescent dyes that absorb in the red over those that absorb at shorter blue and green wavelengths. The most important of these advantages is the reduction in background that ultimately improves the sensitivity achievable. There are three major sources of background: (i) elastic scattering, i.e., Rayleigh scattering, (ii) inelastic scattering, i.e., Raman scattering, and (iii) fluorescence from impurities. The efficiencies of both Rayleigh and Raman scattering are dramatically reduced by shifting to longer wavelength excitation. (scales with the $1/\lambda^4$). Likewise, the number of fluorescent impurities is significantly reduced with longer excitation and detection wavelengths (*6*−*8*). Besides reduced background, a further advantage is that low-cost, energy efficient, rugged diode lasers can be used in place of the more expensive and shorter lived gas lasers. A variety of highly sensitive detectors in the visible-near-IR region are now available. A recent report demonstrated that the use of red-absorbing fluorescent labels and diode laser excitation at 635 nm provides sufficiently low autofluorescence of biological samples so that individual antigen and antibody molecules can be detected in human serum samples (*21*, *22*).

The advantages of red-absorbing fluorophores has prompted current efforts to develop new fluorescent dyes which absorb and emit above 620 nm but still exhibit a sufficient fluorescence quantum yield, especially in an aqueous surrounding (*9*−*11*). Among these new red-absorbing dyes are rhodamine (*10*, *12*), bora-diaza-indacene (*4*, *13*), oxazine (*10*, *14*), squaraine (*15*, *16*), and indocarbocyanine dyes (*17*−*20*). Excitation in the red spectral region is also advantageous when working with live cells because of reduced cell damage (*23*).

Several applications benefit from efficient red-absorbing fluorescent dyes when used in combination with shorter wavelength dyes to increase the spectral range over which detection is possible. In multicolor imaging, the number of simultaneously imaged species can be increased by including red and near-IR absorbing dyes (*24*). Red-absorbing fluorescent dyes are also needed as acceptors in fluorescence resonance energy transfer (FRET) measurements (*25*−*27*). Red-absorbing dyes are also useful in dual-laser fluorescence cross-correlation experiments (*28*, *29*).

The absorption and emission spectra, fluorescence quantum yield, and fluorescence lifetime of dyes often vary with environmental conditions. Thus, many fluorescent dyes can be used as sensors to probe their local environments in biological and analytical applications. For example, coumarin (*30*), rhodamine (*10*, *31*, *32*), oxazine (*33*), and bora-diaza-indacene (*34*) dyes are known to be efficiently quenched by the nucleobase guanosine (dG) and the amino acid tryptophan (Trp). It has been proposed that the mechanism of fluorescence quenching is a photoinduced electron transfer reaction from the guanosine or tryptophan ground-state to the excited singlet state of the dye. The difference between dG or Trp and the other DNA bases and amino acids can

* To whom correspondence should be addressed. Phone: +49-6221-548460, Fax: +49-6221-544255, E-mail: sauer@urz.uni-heidelberg.de.

[†] Universität Heidelberg.

[‡] Florida State University.

10.1021/bc025600x CCC: $25.00
Published on Web 11/27/2002

be attributed to their low oxidation potential (*30*, *35*). Although this quenching effect is not always desirable, it can be used to develop new, highly sensitive probes for the detection of specific DNA sequences (*36*) or proteins (*22*). Others examples of the sensitivity of fluorescent dyes to their local surroundings is the increase in fluorescence intensity and lifetime of some dyes, such as DY-630 and DY-635, upon binding to bovine serum albumin (BSA) (*37*) and the dependence of the cis/trans isomerization rate in some indocarbocyanine dyes on the viscosity of the surrounding medium (*38*, *39*).

An understanding of the dependence of the spectroscopic properties of fluorescent dyes on environmental conditions is crucial for the development of new fluorescence-based assays. Fluorescence quenching effects such as those mentioned above are especially important in fluorescence resonance energy transfer (FRET)-applications, where spectral shifts, fluorescence lifetime, quantum yield changes, and changes in the isomerization rates of the donor or acceptor dye influence the measured FRET efficiencies.

Motivated by these considerations, we studied the spectroscopic characteristics of most of the commercially available fluorescent dyes that absorb and emit in the wavelength range of 640−700 nm and can be conjugated to biological molecules. The fluorescence quantum yield and excited state lifetime of dyes are influenced by the rate of internal conversion, which is controlled by the rigidity of the dye structure (*40*). Since highly viscous solvents impair structural mobility, an increase in fluorescence lifetime and quantum yield is expected with increasing solvent viscosity. The influence of viscosity on the spectroscopic parameters was examined by measuring the spectral properties of the dyes in solvent mixtures of water and glycerin. The influence of solvent polarity on the spectral properties was investigated by comparing measurements in water and ethanol.

To reveal the photophysical properties of the dyes under high excitation conditions, fluorescence correlation spectroscopy (FCS) measurements were performed. FCS permits measurements of a number of photophysical properties of fluorescent dyes such as the triplet lifetime, intersystem crossing yield, photoinduced isomerization, and photobleaching rates (*41*) and is commonly used in fluorescence assays. An often-neglected effect that dramatically influences the achievable detection sensitivity is the hydrophobicity of the dye structure. Very hydrophobic dyes often aggregate or form dimers in aqueous solvents. Therefore, often in fluorescence assays utilizing hydrophobic fluorophores, a detergent such as Tween20 (a nonionic detergent) is included in the buffer to facilitate solvation and prevent dimerization. Consequently, the photophysical characteristics of all red-absorbing fluorescent dyes were also investigated in aqueous medium containing Tween20.

The strong binding of biotin to the 60 kDa protein steptavadin ($K_D = 10^{-15}$ M) has become a standard tool in molecular biology (*42*, *43*). Each hydrophobic binding pocket of streptavidin contains four tryptophan residues that are involved in strong biotin binding (*46*). Because of the importance of the biotin−streptavidin techniques, dyes were covalently attached to biotin and the effect of binding the conjugates to streptavidin was investigated. Quenching or dequenching of the dye's fluorescence upon binding have been observed and were attributed to dye/dye interactions, such as the formation of nonfluorescent dimers or quenching interactions between the dye and the tryptophan-containing binding pocket of streptavidin (*44*, *45*).

EXPERIMENTAL PROCEDURES

Fluorescent Dyes and Conjugates. The dyes used in this study were obtained as *N*-hydroxysuccinimidyl esters. ATTO 655 and ATTO 680 were purchased from ATTO-TEC (Siegen, Germany), Alexa 647, DiD ($DiIC_{18}$ (*5*)), and Bodipy630/650 from Molecular Probes (Göttingen, Germany), Cy5 and Cy5.5 from Amersham Pharmacia Biotech (Freiburg, Germany), and DY-630, DY-635, DY-640, DY-650, DY-655, and EvoBlue30 from Dyomics (Jena, Germany). When dissolved in water, *N*-hydroxysuccinimidyl esters are believed to be deactivated within minutes to hours.

For the biotin−streptavidin studies, the activated dye was coupled with biotin cadaverine (Molecular Probes, Göttingen, Germany) in dimethylformamide with 1% *N*-ethyldiisopropylamine. The reaction solution was incubated for 90 min at room temperature, and the product was purified by HLPC (Hewlett-Packard, Böblingen, Germany) using a reversed-phase column (Knauer, Berlin, Germany) with octadecylsilan-hypersil C18. Separation was performed in 0.1 M triethylammonium acetate, using a linear gradient from 0% to 75% acetonitril in 20 min. Yields >80% were obtained. For coupling to biotin, the dyes Alexa 647 (eluation time: 6.5 min), Bodipy 630/650 (15.0 min), Cy5 (8.9 min), DY-630 (14.5 min), and DY-640 (14.5 min) were used. Biotin conjugates of ATTO 655 (9.3 min) and ATTO 680 (9.5 min) were obtained from ATTO−TEC (Siegen, Germany). All of the dyes, with the exception of DiD, could be linked to biotin−cadaverine in DMF; the HPLC elution time was between the free dye and the activated ester.

Ensemble Spectroscopy. Absorption spectra were taken on a Cary 500 UV−vis−NIR spectrometer (Varian, Darmstadt, Germany). Steady-state fluorescence spectra were measured in standard quartz cuvettes with a LS100 spectrometer (Photon Technology International, Wedel, Germany). Corrected fluorescence spectra were obtained using a high-pressure xenon flash lamp as excitation source. To avoid re-absorption and re-emission effects, concentrations were kept strictly below 1 μM (typically 0.1 μM) in all measurements. Ensemble fluorescence lifetime measurements were performed on a 5000MC spectrometer (IBH, Glasgow, U.K.) using the time-correlated single-photon counting (TCSPC) technique. The excitation source was a pulsed laser diode emitting at 635 nm with a repetition rate of 1 MHz and pulse lengths of ~200 ps (fwhm). With this setup an instrument response function (IRF) of 220 ps (fwhm) was measured. To exclude polarization effects, fluorescence was observed under magic angle (54.7°) conditions. Typically, 5000 photon counts were collected in the maximum channel using 2056 channels (Figure 1). The decay parameters were determined by least-squares deconvolution, and their quality was judged by the reduced χ^2 values and the randomness of the weighted residuals. In the case that a monoexponential model was not adequate to describe the measured decay, a multiexponential model was used to fit the decay (eq 1),

$$I(t) = I(0)\sum a_i \tau_i \qquad (1)$$

where a_i are the preexponential factors that describe the ratio of the excited species and τ_i denote their lifetimes.

Fluorescence Correlation Spectroscopy (FCS). The setup for fluorescence correlation spectroscopy (FCS) measurements has been described recently (*13*). A pulsed diode laser served as excitation source operating at a repetition rate of 64 MHz (PicoQuant, Berlin, Germany).

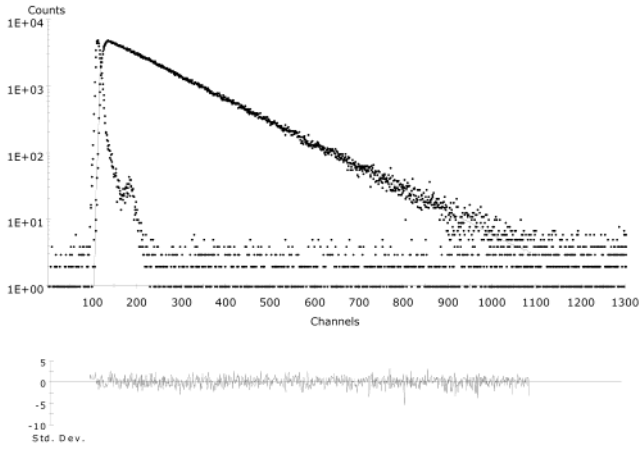

Figure 1. Fluorescence decay of ATTO 680 in EtOH. The instrument response function (IRF), and corresponding fit revealed a monoexponential fluorescence lifetime of 3.04 ns with a reduced χ^2 of 1.160. The weighted residuals of the fit are also shown.

The laser beam passed an excitation filter (639DF9; Omega Optics, Brattleboro, MA) and entered an inverted microscope (Axiovert 100TV, Zeiss, Jena, Germany) through the back port. It was coupled into an oil immersion objective (100×, NA = 1.4, Nikon, Japan) by a dichroic beam splitter (645DLRP, Omega Optics, Brattleboro, MA). The fluorescence signal was collected through the same objective, filtered by two band-pass filters (680HQ60, 675DF50), and imaged onto a 100 μm pinhole diameter directly in front of the avalanche diode (SPAD, AQ 141, EG&G Optoelectronics, Canada). The APD output was connected to a correlator card (model 5000/E, ALV, Langen, Germany). For a correlation curve, 6 runs of 30 s were averaged. All fluorescence measurements were done at room temperature (25 °C).

Data Analysis. Fluorescence intensity autocorrelation functions were calculated by the correlator board and saved as ASCII files. The autocorrelation functions were analyzed with Origin (Microcal Software, Northhampton, MA). Fluorescence correlation spectroscopy (FCS) measures the fluorescence fluctuations arising from fluorescent molecules as they pass the detection volume to obtain information about dynamic processes at the molecular level (*47*). Using FCS, the time dependent fluorescence signal $F = \delta F + \langle F \rangle$ is described by the fluorescence fluctuations $\delta F(t)$ about an average value $\langle F \rangle$. These fluctuations are analyzed in the form of a normalized autocorrelation function $G(\tau)$, where τ denotes the correlation time (eq 2).

$$G(\tau) = \frac{\langle F(t)F(t+\tau)\rangle}{\langle F(t)\rangle^2} = 1 + \frac{\langle \delta F(t)\delta F(t+\tau)\rangle}{\langle F(t)\rangle^2} \quad (2)$$

FCS can be used to gain information about all processes influencing the fluorescence intensity in the detection volume, e.g., translational diffusion, triplet states, or equilibrium constants (*38*, *39*, *41*, *47*).

RESULTS AND DISCUSSION

Absorption and Emission Characteristics of Red-Absorbing Fluorescent Dyes. The molecular structures of some of the investigated dyes are available (Bodipy 630/650, Cy5, Cy5.5, DiD, DY-630, DY-635; see Figure 2), while for other red-absorbing dyes the structures are proprietary (Alexa 647, ATTO 655, ATTO 680, DY-640, DY-650, DY-655, EvoBlue30). Absorption and

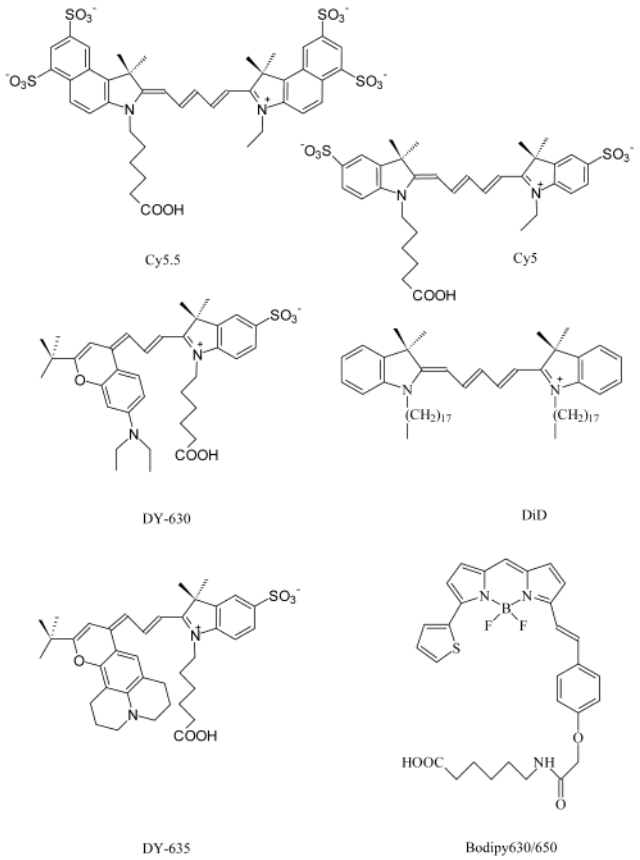

Figure 2. Molecular structures (the free carboxyl group structure without succinimidyl ester) of some of the red-absorbing fluorescent dyes used in this study.

emission maxima of all red-absorbing dyes in different solvents are listed in Table 1. Starting from water, all dyes except DiD show a red-shift in the absorption and emission maximum with increasing glycerol concentration. For most dyes, the absorption and emission maximum is also shifted to the red in ethanol. In contrast, some chromophores, such as ATTO 655, ATTO 680, and DY-640 show distinct shifts to shorter wavelengths in ethanol, especially for the absorption maxima.

Due to long alkyl side chains (C_{18}) and the lack of sulfonate groups, the carbocyanine dye DiD shows a strong aggregation tendency in aqueous solvents which promotes the formation of nonfluorescent dimers and aggregates. DiD and related dyes exhibit a strong fluorescence increase when incorporated into membranes (*48*), organic solvents, or immobilized on dry glass surfaces (*49*). The addition of 0.05% (v/v) Tween20 reduces the aggregation tendency and increases the fluorescence lifetime and intensity significantly (Table 1). The absorption and emission characteristics of dyes of the DY-family are also strongly influenced by the addition of Tween20. For example, the absorption maximum of DY-635 is 16 nm red-shifted from 635 to 651 nm upon addition of the detergent.

Figure 3 shows the retention times of the red-absorbing dyes measured by HPLC on a reversed-phase column using a water/acetonitrile gradient. The measured retention times suggest the classification of the dyes into two groups: hydrophilic dyes (Alexa 647, ATTO 655, ATTO 680, Cy5, Cy5.5, and EvoBlue30) and hydrophobic dyes (DiD, Bodipy 630/650, and the dyes of the DY-family). In general, the more hydrophobic chromophores are influenced by the addition of Tween20 while more hydrophilic dyes are not. The spectroscopic data of the

Table 1. Spectroscopic Characteristics (absorption maxima, λ_{abs} (nm), Emission Maxima, λ_{em} (nm), and Fluorescence Lifetimes, τ (ns)) of Red-Absorbing Fluorescent Dyes in Different Solvents[a,b]

	λ_{abs} (nm)/λ_{em} (nm)/τ (ns)												
	Alexa 647	ATTO 655	ATTO 680	Bodipy630/650	Cy5	Cy5.5	DiD[c]	DY-630	DY-635	DY-640	DY-650	DY-655	EVOblue30
water	649	661	680	629	647	675	652	627	635	627	646	637	650
	666	678	695	646	663	692	–	651	669	667	670	676	667
	1.04	1.87	1.69	3.89	0.91	0.83	–	0.21	0.48	0.59	0.64	0.54	0.64
20%	652	664	682	631	649	677	649	629	640	628	649	641	653
glycerol	667	680	699	648	666	695	–	653	668	662	668	683	670
	1.22	2.02	1.83	4.01	1.13	1.03	–	0.36	0.72	0.84	0.97	0.79	0.79
40%	654	666	685	633	652	680	648	632	644	631	650	646	655
glycerol	670	683	701	648	669	698	–	655	669	667	674	683	673
	1.44	2.17	1.96	4.06	1.39	1.27	–	0.62	0.99	1.19	1.28	1.09	1.01
ethanol	655	655	675	628	652	685	647	636	647	624	654	645	649
	674	677	695	643	672	706	668	657	671	651	675	672	666
	1.51	3.31	3.04	4.42	1.32	1.23	1.12	0.30	0.98	3.33	0.95	0.97	1.16
0.05%	649	661	680	633	647	675	648	637	651	628	656	648	650
Tween20	665	677	694	648	663	692	667	660	675	659	676	680	667
	1.03	1.87	1.68	4.96	0.92	0.86	1.62	0.94	1.66	3.64	1.82	2.07	0.66

[a] The extinction coefficients reported by the manufacturers, ϵ (L mol^{-1} cm^{-1}) are 2.5×10^5 for Cy5, Cy5.5, and Alexa 647, 0.97×10^5 for Bodipy630/650, $>1.2 \times 10^5$ for DY-630 and DY-635, 2.6×10^5 for DiD, and 1.0×10^5 for ATTO 655 and ATTO 680. [b] The quality of the fit was judged by the reduced χ^2 values and the randomness of the weighted residuals (Figure 1). For all fits, χ^2 values between 0.900 and 1.200 were obtained. Viscosities of the solvents at 20 °C are 1.00 mPa s (water), 2.025 mPa s (20% glycerol, v/v), 4.95 mPa s (40% glycerol, v/v), and 1.2 mPa s (ethanol). Fluorescent dyes of the DY-family show only weak fluorescence intensity and nonexponential fluorescence kinetics. Therefore average fluorescence lifetimes, $\tau_{av} = a_1\tau_1 + a_2\tau_2$, are given. [c] The carbocyanine dye DiD shows a strong aggregation tendency in aqueous solvents which promotes the formation of nonfluorescent dimers or aggregates.

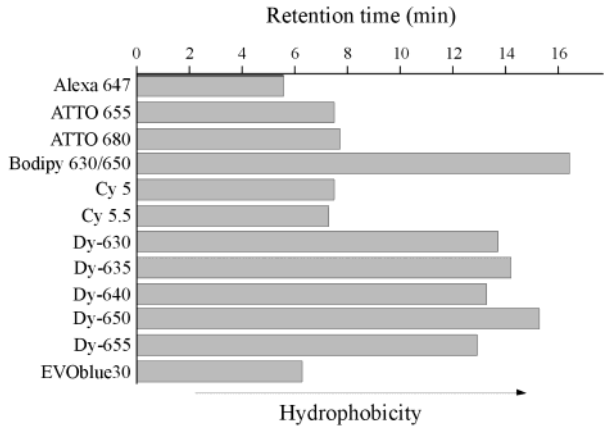

Figure 3. Retention times of red-absorbing fluorescent dyes measured by HPLC. The dye DiD did not elute under the applied experimental conditions. Separation was performed in 0.1 M triethylammonium acetate, using a linear gradient from 0% to 75% acetonitril in 20 min.

hydrophobic bora-diaza-indacene dye Bodipy 630/650 are nearly unaffected by the surrounding medium (Table 1).

Neglecting the dielectric constant, ϵ, dye-solvent interactions are, in general, described by the refractive index of the solvent, n, if the interactions are predominated by dispersion forces (*50*). Generally, an increase of the refractive index is expected to result in a red-shift of the absorption maximum. The refractive indices of the solvents used in our experiment are 1.33 (water), 1.36 (ethanol), 1.36 (20% glycerol in water), and 1.40 (40% glycerol in water). As can be seen from Table 1, the absorption and emission maxima of all dyes investigated show a red-shift with increasing glycerol concentration. Using ethanol as the solvent also increases the refractive index, but the effect on the absorption and emission spectra is less pronounced. This, and the fact that some dyes (ATTO 655, ATTO 680, EVOblue30, and Bodipy 630/650) show a blue-shift in ethanol mixtures means that other effects, such as the polarity and the solvation of the different chromophore structures must also influence the absorption and emission maxima.

Fluorescence Lifetimes of Red-Absorbing Fluorescent Dyes. Due to problems associated with adsorption of hydrophobic dyes to the walls of the quartz cuvettes, we have not attempted to report the measured values of the fluorescence quantum yields. However, since the fluorescence quantum yield, Φ_f, is defined as $\Phi_f = \tau/\tau_n$ in the absence of static fluorescence quenching (τ_n: native radiative lifetime without any nonradiative processes), an increase or decrease in the measured fluorescence lifetime is always related to an increase or decrease in fluorescence quantum yield.

Figure 4 shows the relative fluorescence lifetimes (relative to pure water value) measured for each dye in each of the various solvent conditions tested. On the basis of the dependence of the fluorescence lifetime on the different solvents, the red-absorbing dyes investigated in this study can be divided into the following groups: (i) fluorescent dyes for which the lifetime is independent of the surrounding medium (Bodipy 630/650), (ii) fluorescent dyes for which the lifetime is much longer in ethanol than water, but does not change significantly in the presence of Tween20 (ATTO 655, ATTO 680, Alexa 647, EVOblue30, Cy5, and Cy5.5.; see Figure 4A), and (iii) fluorescent dyes from the DY-family for which the lifetime is much longer with Tween20 than in pure water. Within these groups there are still some differences: For example, the fluorescence lifetimes of ATTO 655, ATTO 680, and EVOblue30 dyes are less sensitive to solvent viscosity, e.g., in 40% glycerol, than they are to solvent polarity (ethanol). These observations, especially the strong increase in fluorescence lifetime of ATTO 655, ATTO 680, and EvoBlue30 in ethanol, indicate a more rigid chromophore structure. It was recently shown that several red-absorbing rhodamine and oxazine dyes (both xanthene dyes with rigid structures) exhibit shorter fluorescence lifetimes in water than in ethanol (*3*, *10*). On the other hand, the viscosity (and temperature) dependence of the fluorescence characteristics is only weak. From these findings, we assume that the three red-absorbing fluorescent dyes ATTO 655, ATTO 680, and EVOblue30 have a rigid planar chromophore structure which do not show cis/trans isomerization processes

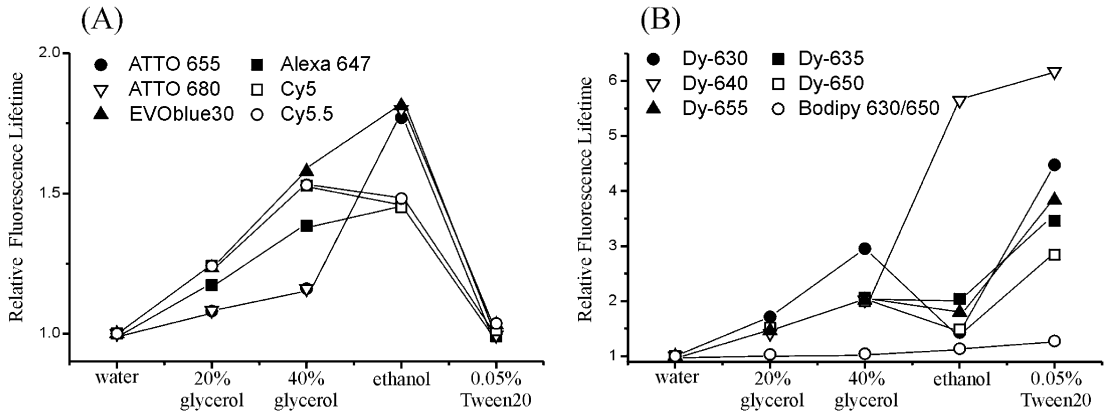

Figure 4. Relative fluorescence lifetimes measured for the red-absorbing fluorescent dyes in different solvents. Relative fluorescence lifetimes were calculated by dividing the measured values by the value obtained in water.

commonly observed for chromophores with flexible polymethine groups.

The other three dyes of this group (Figure 4A), Alexa 647, Cy5, and Cy5.5 show shorter fluorescence lifetimes but otherwise absolutely identical dependencies. Due to the flexibility of the polymethine backbone of carbocyanine dyes and consequential cis/trans isomerization possibilities, the fluorescence lifetimes and quantum yields are strongly influenced by the viscosity (Figure 4A). This is in good agreement with earlier findings for most cyanine dyes at room temperature in alcoholic or aqueous solutions which demonstrated that viscosity is the dominating solvent property influencing the fluorescence intensity and that the polarity of the solvent plays only a minor role (*51*). As expected for more hydrophilic dyes (Figure 3), the fluorescence properties of all red-absorbing fluorescent dyes of this group (Figure 4A) are very weakly influenced by the addition of 0.05% Tween20 (v/v) to an aqueous solution.

The fluorescent dyes from the DY-family (Figure 4B) all show a similar increase in fluorescence lifetime upon changing the solvent from water to water/glycerol mixtures or pure ethanol. Only for the dye DY-640, both the viscosity and the polarity strongly influence the fluorescence intensity and lifetime to the same degree (see lifetimes in ethanol and upon addition of Tween20). Nevertheless, the strong increase in fluorescence lifetime and intensity upon addition of 0.05% Tween20 (v/v) to an aqueous solution (up to 6-fold) is unexpected. Certainly, the addition of Tween20 reduces the aggregation tendency and promotes the solubility of these rather hydrophobic dye structures in aqueous solutions (Figure 3), but the degree of this increase in fluorescence intensity indicates that other effects have to be taken into account. For example, as can be seen in Figure 2, at least two dyes of the DY-family are asymmetric carbocyanine dyes (DY-630, DY-635). It may be that those dyes associate with Tween20 molecules or micelles thereby increasing the solubility and decreasing the internal conversion rate by reducing the flexibility of the polymethine backbone.

Fluorescence Correlation Spectroscopy (FCS) Measurements. The dyes used in this study, particularly the more hydrophobic dyes, show dynamic adsorption on the cover slides used for FCS measurements. Furthermore, some dyes show strong adsorption to nonfluorescent impurities, e.g., dust particles, in aqueous solutions. These problems render the analysis of the normalized autocorrelation functions more difficult. Therefore, experiments were performed in water containing 0.05% Tween20 (v/v), which effectively eliminates these problems.

In FCS measurements, transient nonfluorescent states such as triplet states or cis-conformations (as in the case of the carbocyanine dye Cy5) (*38*) give rise to fluorescence fluctuations that are superimposed on those caused by 3D-translational motion (Brownian motion) of the fluorescent molecule in and out of the sample volume element. Since the lifetime of these transient states are usually shorter, i.e., in the range of several microseconds, than the typical diffusion time of a fluorescent dye molecule through the sample volume element, they can be analyzed separately (*41*). While translational diffusion is, as a first approximation, independent of the laser excitation energy (neglecting photobleaching effects), intersystem crossing and photoinduced cis/trans isomerization is not. Widengren and Schwille recently showed that the correlation times for cis/trans isomerization for the carbocyanine dye Cy5 are drastically reduced with higher excitation intensities but that the amplitude of this process (about 50%) is not excitation power dependent (*38*).

Figure 5 shows representative FCS curves of the red-absorbing fluorescent dyes for a range of excitation intensities in water containing 0.05% Tween20 (v/v). In these experiments, four different types of FCS curves and excitation intensity dependencies were observed. The FCS curves obtained for EVOblue30 under various excitation intensities (Figure 5A) are representative for FCS curves measured for ATTO 655, ATTO 680. They are also representative for Bodipy 630/650, except that Bodipy 630/650 has a slightly longer diffusion time. FCS curves of these fluorescent dyes can be described exclusively by translational diffusion up to an excitation energy of 100 kW/cm^2. This indicates that the intersystem crossing yield is very low under moderate excitation conditions. Figure 5B shows the FCS curves measured for DY-640 under various excitation intensities. Similar curves were obtained for DY-655. For these dyes, a second exponential process could be observed at excitation intensities of >27 kW/cm^2 with an amplitude of 30−35% (at 100 kW/cm^2). This second process can be ascribed to intersystem crossing into the triplet state. In addition, at excitation intensities above 27 kW/cm^2 a distinctly faster decay of the autocorrelation curves due to photobleaching is evident.

The normalized intensity autocorrelation curves presented in Figure 5C are representative for carbocyanine dyes showing photoinduced cis/trans isomerization. These

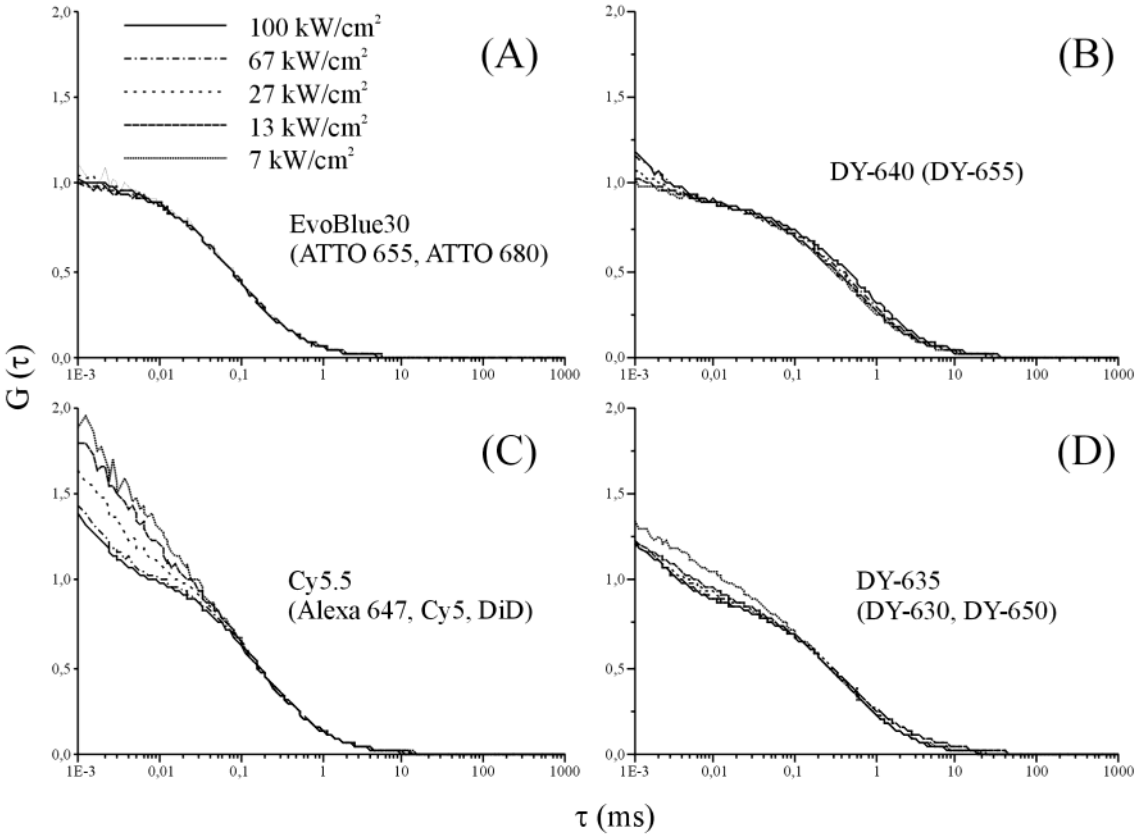

Figure 5. FCS curves of some red-absorbing fluorescent dyes in water containing 0.05% Tween20 (v/v) at excitation intensities of 7, 13, 27, 67, and 100 kW/cm². (A) EVOblue30; similar curves were obtained for ATTO 655, ATTO 680 and, with a longer diffusion time, for Bodipy 630/650. (B) DY-640; similar traces were obtained for DY-655. (C) Cy5.5; similar curves were obtained for Alexa 647, Cy5 and DiD. (D) DY-635; similar curves were obtained for DY-630 and DY-650.

dyes, Cy5, Cy5.5, DiD, and Alexa 647, all show identical excitation intensity dependence in FCS curves. The relaxation times for cis/trans isomerization are drastically reduced with higher excitation intensities. At the highest excitation intensity (100 kW/cm²) weak triplet state population is observed. Although the molecular structure of Alexa 647 has not been published, the FCS curves and fluorescence lifetimes strongly indicate that it has a carbocyanine structure. For DiD, significant photobleaching, manifested by faster decays of the FCS curves for excitation intensities above 20 kW/cm², is evident.

The FCS curves recorded for DY-630, DY-635, and DY-650 under various excitation intensities (Figure 5D) exhibit behavior similar to those shown in Figure 5C. The major difference is that a second component (other than translational diffusion) is required to describe the curves even under weak excitation conditions. Besides the apparent photobleaching at higher excitation intensities, the more hydrophobic red-absorbing dyes, especially the dyes of the DY-family shown in Figs. 5B and 5D and Bodipy630/650, show slower translational diffusion. This implies that those dyes tend to adsorb to Tween20 micelles, which increases the observed diffusion time.

To summarize, the best signal-to-noise ratios in the FCS measurements were obtained for all dyes applying an excitation intensity of 67 kW/cm². For our excitation wavelength and filter combination, Alexa 647, Cy5, ATTO 655, DY-640, and Bodipy 630/650 proved to be the brightest red-absorbing fluorescent dyes in aqueous solutions containing 0.05% Tween 20. Since the cis and triplet states of dyes such as Cy5, Cy5.5, or Alexa 647 are also potential nonfluorescent energy transfer acceptors, the use of these dyes as acceptors in FRET measurements is more problematic (*39*, *52*). Due to their low intersystem crossing yields, ATTO 655, ATTO 680, DY-640, and Bodipy 630/650 offer efficient alternatives. Fluorescent dyes of the DY-family require the addition of detergents to compete.

Biotin Conjugates and Streptavidin Binding. The steady-state absorption and fluorescence spectra of the biotin conjugates of Alexa 647, ATTO 655, ATTO 680, Cy5, DY-630, and DY-640 are all shifted slightly to the red compared to the free dyes (Table 2). In addition, most biotin conjugated dyes exhibit a slight increase in fluorescence lifetime. However, the absorption and fluorescence excitation spectra of the Bodipy 630/650 biotin conjugate indicate the formation of nonfluorescent dimers. From the data shown in Table 2, it is clear that the addition of streptavidin significantly alters the spectroscopic properties of all conjugates investigated. To prevent dye/dye interactions between biotin conjugated dyes bound to neighboring binding sites of the same streptavidin, an excess of streptavidin was used (*44*). Carbocyanine dyes such as Cy5 show bathochromic shifts in absorption and emission and a considerable increase in fluorescence lifetime. The fact that Cy5 and Alexa 647 both show this behavior is another indicator that they are similar in structure. The two conjugates from the DY-family (DY-630, DY-640) show a strong increase in fluorescence lifetime and intensity upon addition of streptavidin. The fluorescence decays of the DY-630 and DY-640 biotin conjugates show a second dominant component with a long fluorescence lifetime, similar to the fluorescence lifetimes obtained upon addition of Tween20 to an aqueous solution of the free dyes. Surprisingly, the emission maximum of the DY-640 biotin conjugate showed a 10 nm blue-shift upon addition of streptavidin.

Table 2. Spectroscopic Characteristics (Absorption Maxima, λ_{Abs} (nm), Emission Maxima, λ_{em} (nm), Fluorescence Lifetimes, τ (ns)) of Dye−Biotin Conjugates in the Absence/Presence of an Excess of Streptavidin in Water[a]

	λ_{abs} (nm)	λ_{em} (nm)	τ_1 (ns)	a_1	τ_2 (ns)	a_2
Alexa 647	649/655	667/669	1.24/0.98	1.00/0.67	−/1.96	−/0.33
ATTO 655	662/667	677/677	2.06/2.01	1.00/0.86	−/0.34	−/0.14
ATTO 680	681/687	701/700	1.84/1.79	1.00/0.74	−/0.35	−/0.26
Bodipy 630/650	645*/635	650/662	3.82/3.11	1.00/0.85	−/0.54	−/0.15
Cy5	647/653	664/668	1.07/1.84	1.00/1.00	−/−	−/−
Dy-630	629/634	652/654	0.30/0.77	0.44/0.30	0.59/1.74	0.56/0.70
Dy-640	630/631	667/657	0.74/0.57	0.96/0.05	2.06/3.87	0.05/0.95

[a] The quality of the fit was judged by the reduced χ^2 values and the randomness of the weighted residuals. Most biotin conjugates show a biexponential fluorescence decay upon binding to streptavidin.

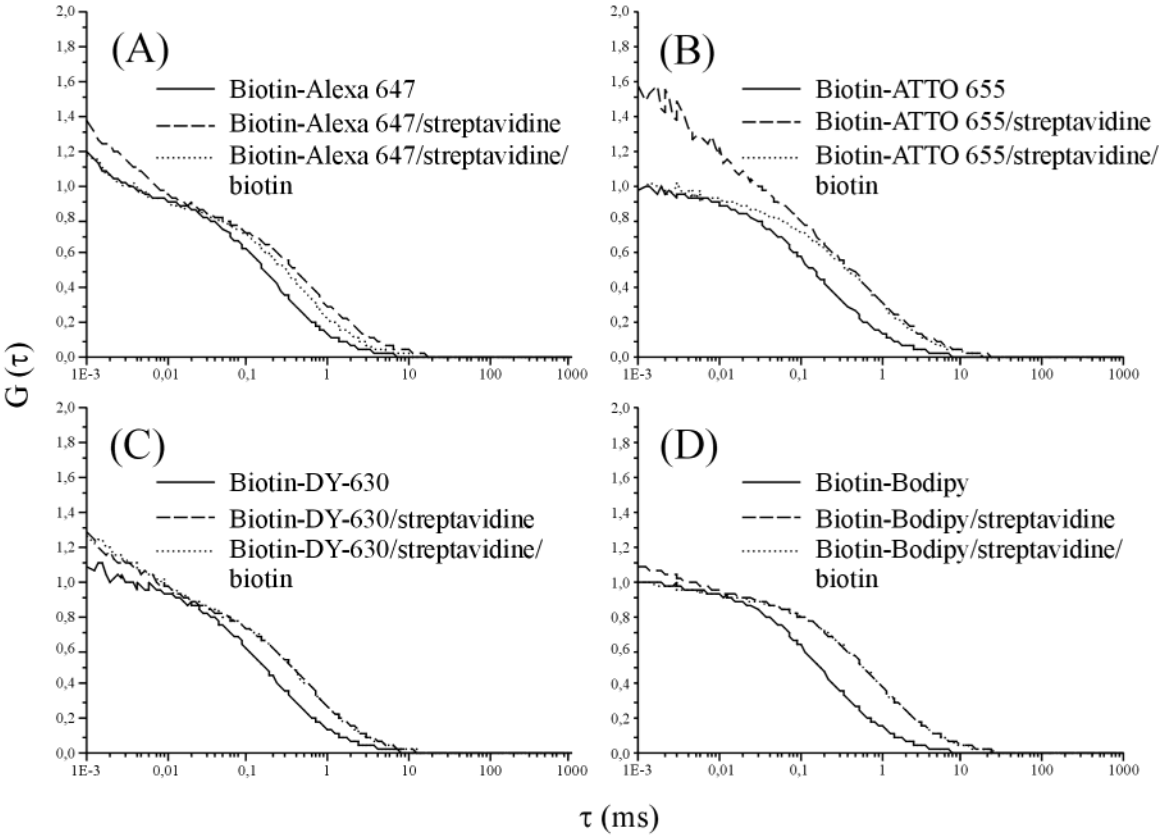

Figure 6. FCS curves of some biotin conjugates in water measured at an excitation intensity of 67 kW/cm^2. The solid lines give the FCS curves of the biotin conjugates, the dashed line upon addition of an excess of streptavidin, and the dotted line upon a subsequent addition of an excess of unlabeled biotin. (A) Biotin−Alexa 647, similar curves were obtained for Cy5. (B) Biotin−ATTO 655, similar curves were obtained for ATTO 680. (C) Biotin−DY-630, similar curves were obtained for DY-640. (**D**) Biotin−Bodipy 630/650.

In contrast, the biotin conjugates of ATTO 655, ATTO 680, and Bodipy 650/680 show fluorescence quenching upon addition of an excess of streptavidin, indicated by the appearance of a shorter component in the fluorescence decay (Table 2). In the case of the Bodipy 630/650 biotin conjugate, the dimers disappear completely upon binding to streptavidin.

Figure 6 shows FCS curves recorded for some biotin conjugates in water with and without the addition of an excess of streptavidin (solid line and dashed line, respectively). The binding of the biotin conjugates to streptavidin can be confirmed and monitored by the shift of the diffusional correlation times. Because we want to observe this shift, these measurements were performed in pure water, i.e., without Tween20.

Upon addition of streptavidin, all the FCS curves showed an increased translational diffusion time, confirming that streptavidin binds each dye conjugate. The FCS curves also showed additional fast correlation times in the presence of an excess of streptavidin for all biotin-conjugated dyes. For example, biotin conjugates of Alexa 647 (Figure 6A) and DY-630 (Figure 6C) that show the expected short correlation times due to cis/trans isomerization and intersystem crossing in the absence of streptavidin show an increase of the short correlation terms after streptavidin binding in the short-times range. In almost the same manner, the FCS curves of the Bodipy 630/650 conjugates show an additional term in the short time range in the presence of streptavidin (Figure 6D). However, the biotin conjugates of ATTO 655 and ATTO 680 show the most pronounced changes upon addition of streptavidin (Figure 6B, FCS curves for ATTO 655). The data shown in Table 2 indicate fluorescence quenching of the dye due to binding of the biotin conjugate to streptavidin. This quenching correlates with the appearance of the additional short-time FCS decay components.

It is likely that the additional short correlation times observed in the FCS curves upon streptavidin binding is caused by reversible quenching of the dye with tryptophan residues of streptavidin. The quenching could be from tryptophan residues at the streptavidin binding site, or from one (or more) of the three neighboring, unoc-

cupied binding sites. To distinguish these two possibilities, an excess of unlabeled biotin was added. The addition of excess free biotin blocks neighboring binding sites and suppresses possible interactions between the dye and those tryptophan residues. Another possible process to consider is that unlabeled and labeled biotins compete for the same streptavidin binding sites, i.e., dye-labeled biotin may be displaced (*42*−*45*). The FCS curves of the biotin conjugates of hydrophobic dyes (DY-630, DY-640, Bodipy 630/650; see Figures 6C and 6D) do not change upon addition of excess free biotin, but the conjugates of more hydrophilic dyes such as Alexa 647, Cy5, ATTO 655, and ATTO 680 do show a decrease in the translational diffusion times (Figures 6A and 6B).

Hydrophilic dyes bind in the binding pocket, hence they can be displaced by competing free biotin; hydrophobic dyes bind nonspecifically, i.e., not at the binding sites, therefore they are not displaced by free biotin.

With the exception of DY-630 and DY-640 (Figure 6C), the additional short-time FCS decay component disappears when an excess of biotin is added to the streptavidin−biotin-dye complexes. The disappearance of the additional fast process for Alexa 647, Cy5, ATTO 655, ATTO 680, and Bodipy 630/650 indicates that these dyes interact with neighboring binding sites, likely with the tryptophan residues, that are inhibited upon addition and binding of unlabeled biotin molecules. In the case of ATTO 655, ATTO 680, and Bodipy 630/650, the quenching probably occurs via an electron transfer reaction from the ground state tryptophan residue to the first excited singlet state of the dye (*22*, *33*, *34*, *36*). Since carbocyanine dyes such as Cy5 exhibit a lower electron accepting tendency, they are not quenched (*14*). The loss of the additional short-time component for the Alexa 647 and Cy5 streptavidin complexes in excess free biotin are not easily explained. It is likely that the observed changes are related to a change in the cis/trans isomerization rate brought on by a conformational change that occurs when the neighboring binding sites are filled. The reason that the additional short-time FCS decay components do not disappear on addition of free biotin for DY-630 and DY-640 conjugates is that these biotin−dye complexes are in fact bound to streptavidin nonspecifically through hydrophobic interactions of the dye and the protein interior. As a result, the binding to streptavidin is independent of whether free biotin is present at the streptavidin binding sites.

CONCLUSIONS

The spectroscopic data of 13 commercially fluorescent dyes absorbing in the red-wavelength range (620−700 nm)—a very promising wavelength range for diagnostic applications—are measured and compared using ensemble steady-state and time-resolved fluorescence spectroscopy as well as fluorescence correlation spectroscopy (FCS). The best signal-to-noise ratios in aqueous solutions are obtained for the relatively hydrophilic dyes Cy5, Cy5.5, Alexa 647, ATTO 655, and ATTO 680. The data obtained strongly suggest that besides Cy5 and Cy5.5, Alexa 647 also belongs to the class of symmetric carbocyanine dyes which show excitation intensity dependent cis/trans isomerization and short fluorescence lifetimes of ∼1 ns in aqueous solutions. Due to their similar spectroscopic behavior, the red-absorbing dyes EVOblue30 and the two ATTO-dyes probably belong to the same class of structurally rigid chromophores such as rhodamines or oxazines. ATTO 655 and ATTO 680 exhibit longer fluorescence lifetimes in aqueous solutions than the carbocyanine dyes, thus allowing an improved discrimination against autofluorescent impurities which normally have very fast fluorescence decays. On the other hand, both chromophore classes might be used to probe the local environment due to specific quenching processes or changes in the cis/trans isomerization rates. Although the fluorescence intensity and lifetime of Bodipy 630/650 is superior and nearly independent of the surrounding medium, the strong dimerization and nonspecific adsorption tendency renders its application more difficult in aqueous solutions. The relatively hydrophobic fluorescent dyes of the DY-family proved to be only weakly fluorescent in aqueous solutions. However, upon addition of Tween20 or binding of biotin conjugates to streptavidin, the fluorescence drastically increases.

The results presented demonstrate that knowledge of the spectroscopic behavior of the dyes used under various conditions is crucial for the design of any application. As an example, the binding of labeled biotin conjugates to streptavidin was monitored. Selective fluorescence quenching of dyes by tryptophan residues in proteins has great potential for the development of diagnostic applications (*22*). Furthermore, the data show that changes in the fluorescence lifetime of the dye or any other photophysical properties such as cis/trans isomerization might be used advantageously in developing fluorescence-based assays. Finally, the data suggest that the fluorescent dye that exhibits the highest signal-to-noise ratio is not necessarily the best dye for any desired application. It is also important to consider experimental details such as the excitation intensity, the optimum solvent conditions, and the protein/peptide or DNA/RNA sequence of the probe or target molecule.

ACKNOWLEDGMENT

This work was supported by the Bundesministerium für Bildung, Wissenschaft, Forschung und Technologie (Grant 311864).

LITERATURE CITED

(1) Smith, L. M., Fung, S., Hunkapillar, M. W., and Hood, L. E. (1985) The synthesis of oligonucleotides containing an aliphatic amine group at the 5′-terminus: synthesis of fluorescent DNA primers for use in DNA sequence analysis. *Nucleic Acids Res. 13*, 2328−2410.

(2) Waggoner, A. (1995) Covalent labeling of proteins and nucleic acids with fluorophores. In *Methods in Enzymology* (Abelson, J. N., and Simon, M. I., Eds.) Vol. 246, pp 362−373, Academic Press, San Diego, CA.

(3) Daehne, S. (1998) Near-infrared dyes for high technology applications. Kluwer, Dordrecht.

(4) Haugland, R. P. (1996) Handbook of fluorescent probes and research chemicals, Sixth Edition, Molecular Probes, Eugene.

(5) Hovius, R., Vallotton, P., Wohland, T., and Vogel, H. (2000) Fluorescence techniques: shedding light on ligand acceptor interactions. *Trends Pharmacol. Sci. 21*, 266−273.

(6) Aubin, J. E. (1979) Autofluorescence of viable cultured mammalian cells. *J. Histochem. Cytochem. 27*, 35−43.

(7) Cheng, P. C., and Kriete, A. (1995) Image contrast in confocal light microscopy. In *Handbook of biological confocal microscopy* (Pawley, J. B., Ed.) 2nd ed., pp 327−346, Plenum Press, New York.

(8) Affleck, R. L., Ambrose, W. P., Demas, J. N., Goodwin, P. M., Schecker, J. A., Wu, M., and Keller, R. A. (1996) Reduction of luminescent background in ultrasensitive fluorescence detection by photobleaching. *Anal. Chem. 68*, 2270−2276.

(9) Patonay, G., and Antoine, M. D. (1991) Near-infrared fluorogenic labels: New approach to an old problem. *Anal. Chem. 63*, 321A−327A.

(10) Sauer, M., Han, K. T., Ebert, V., Müller, R., Schulz, A., Seeger, S., Wolfrum, J., Arden-Jacob, J., Deltau, G., Marx,

N. J., Zander, C., and Drexhage, K. H. (1995) New fluorescent dyes in the red region for biodiagnostics. *J. Fluoresc. 5*, 247−261.

(11) William, D. C., and Soper, S. A. (1995) Ultrasensitive near-IR fluorescence detection for capillary gel electrophoresis and DNA sequencing applications. *Anal. Chem. 67*, 3427−3432.

(12) Arden-Jacob, J., Marx, N. J., and Drexhage, K. H. (1997) New fluorescent probes for the red spectral region. *J. Fluoresc. 7*, 91S−93S.

(13) Sauer, M., Arden-Jacob, J., Drexhage, K. H., Göbel, F., Lieberwirth, U., Mühlegger, K., Müller, R., Wolfrum, J., and Zander, C. (1998) Time-resolved identification of individual mononucleotide molecules in aqueous solution with pulsed semiconductor lasers. *Bioimaging 6*, 14−24.

(14) Lieberwirth, U., Arden-Jacob, J., Drexhage, K. H., Herten, D. P., Müller, R., Neumann, M., Schulz, A., Siebert, S., Sagner, G., Klingel, S., Sauer, M., and Wolfrum, J. (1998) Multiplex dye DNA sequencing in capillary gel electrophoresis by diode laser-based time-resolved fluorescence detection. *Anal. Chem. 70*, 4771−4779.

(15) Terpetschnig, E., Szmacinski, H., Ozinskas, A., and Lakowicz, J. R. (1994) Synthesis of squaraine-N-hydroxysuccinimide esters and their biological application as long-wavelength fluorescent labels. *Anal. Biochem. 217*, 197−204.

(16) Oswald, B., Patsenker, L., Duschl, J., Szmacinski, H., Wolfbeis, O. S., and Terpetschnig, E. (1999) Synthesis, spectral properties, and detection limits of reactive squaraine dyes, a new class of diode laser compatible fluorescent protein labels. *Bioconjugate Chem. 10*, 925−931.

(17) Mujumdar, R. B., Ernst, L. A., Mujumdar, S. R., and Waggoner, A. S. (1989) Cyanine dye labeling reagents containing isothiocyanate groups. *Cytometry 10*, 11−19.

(18) Southwick, P. L., Ernst, L. A., Tauriello, E. V., Parker, S. R., Mujumdar, R. B., Mujumdar, S. R., Clever, H. A., and Waggoner, A. S. (1990) Cyanine dye labeling reagents: carboxymethylinindocyanine esters. *Cytometry 11*, 418−430.

(19) Mujumdar, R. B., Ernst, L. A., Mujumdar, S. R., Lewis, C. J., and Waggoner, A. S. (1993) Cyanine dye labeling reagents: Sulfoindocyanine succinimidyl esters. *Bioconjugate Chem. 4*, 105−111.

(20) Flanagan, J. H., Jr., Khan, S. H., Menchen, S., Soper, S. A., and Hammer, R. P. (1997) Functionalized tricarbocyanine dyes as near-infrared fluorescent probes for biomolecules. *Bioconjugate Chem. 8*, 751−756.

(21) Sauer, M., Zander, C., Müller, R., Ullrich, B., Drexhage, K. H., Kaul, S., and Wolfrum, J. (1997) Detection and identification of individual antigen molecules in human serum with pulsed semicoductor lasers. *Appl. Phys. B 65*, 427−431.

(22) Neuweiler, H., Schulz, A., Vaiana, A., Smith, J., Kaul, S., Wolfrum, J., and Sauer, M. (2002) Peptide-based molecular beacons for the detection of p53-autoantibodies in human sera. *Angew. Chemie*, in press.

(23) Terasaki, M., and Dailey, M. E. (1995) Confocal microscopy on living cells. In *Handbook of biological confocal microscopy* (Pawley, J. B., Ed.) 2nd ed., pp 327−346, Plenum Press, New York.

(24) Sawano, A., Hama, H., Saito, N., and Miyawaki, A. (2002) Multicolor imaging of Ca^{2+} and protein kinase C signals using novel epifluorescence microscopy: *Biophys. J. 82*, 1076−1085.

(25) Förster, T. (1949) Experimentelle und theoretische Untersuchung des zwischenmolekulares Übergangs von Elektronenanregungsenergie. *Z. Naturforsch. 4a*, 321−327.

(26) Weiss, S. (1998) Fluorescence spectroscopy of single biomolecules. *Science 283*, 1676−1683.

(27) Gordon, G. W., Berry, G., Liang, X. H., Levine, B., and Herman, B. (1998) Quantitative fluorescence resonance energy transfer measurements using fluorescence microscopy. *Biophys. J. 74*, 2702−2713.

(28) Schwille, P., Meyer-Almes, F. J., and Rigler, R. (1997) Dual-color fluorescence cross-correlation spectroscopy for multicomponent diffusional analysis in solution. *Biophys. J. 72*, 1878−1886.

(29) Hom, E. F. Y., and Verkman, A. S. (2002) Analysis of coupled bimolecular reaction kinetics and diffusion by two-color fluorescence correlation spectroscopy: Enhanced resolution of kinetics by resonance energy transfer. *Biophys. J. 83*, 533−546.

(30) Seidel, C. A. M., Schulz, A., and Sauer, M. (1996) Nucleobase-specific quenching of fluorescent dyes. 1. Nucleobase one-electron redox potentials and their correlation with static and dynamic quenching efficiencies. *J. Phys. Chem. 100*, 5541−5553.

(31) Edman, L., Mets, Ü., and Rigler, R. (1996) Conformational transitions monitored for single molecules in solution. *Proc. Natl. Acad. Sci. U.S.A. 93*, 6710−6715.

(32) Eggeling, C., Fries, J. R., Brand, L., Günther, R., and Seidel, C. A. M. (1998) Monitoring conformational dynamics of a single molecule by selective fluorescence spectroscopy. *Proc. Natl. Acad. Sci. U.S.A. 95*, 1556−1561.

(33) Sauer, M., Drexhage, K. H., Lieberwirth, U., Müller, R., Nord, S., and Zander, C. (1998) Dynamics of the electron-transfer reaction between an oxazine dye and DNA oligonucleotides monitored at the single molecule level. *Chem. Phys. Lett. 284*, 153−163.

(34) Kurata, S., Kanagawa, T., Yamada, K., Torimura, M., Yokomaku, T., Kamagata, Y., and Kurane, R. (2001) Fluorescent quenching-based quantitative detection of specific DNA/RNA using BODIPY FL-labeled probe or primer. *Nucleic Acids Res. 29*, e34.

(35) Wagenknecht, H. A., Stemp, E. D. A., and Barton, J. K. (2000) Evidence of electron transfer from peptides to DNA: Oxidation of DNA-bound tryptophan using the flash-quench technique. *J. Am. Chem. Soc. 122*, 1−7.

(36) Knemeyer, J. P., Marmé, N., and Sauer, M. (2000) Probes for the detection of specific DNA sequences at the single-molecule level. *Anal. Chem. 72*, 3717−3724.

(37) Czerney, P., Lehmann, F., Wenzel, M., Buschmann, V., Dietrich, A., and Mohr, G. J. (2001) Tailor-made dyes for fluorescence correlation spectroscopy (FCS). *Biol. Chem. 382*, 495−498.

(38) Widengren, J., and Schwille, P. (2000) Characterization of photoinduced isomerization and back-isomerization of the cyanine dye Cy5 by fluorescence correlation spectroscopy. *J. Phys. Chem. A 104*, 6416−6428.

(39) Widengren, J., Schweinberger, E., Berger, S., and Seidel, C. A. M. (2001) Two new concepts to measure fluorescence resonance energy transfer via fluorescence correlation spectroscopy: Theory and experimental realizations. *J. Phys. Chem. A 105*, 6851−6866.

(40) Drexhage, K. H. (1973) Structure and properties of laser dyes. In *Dye Lasers* (Schäfer, F. P., Ed.), pp 144−193, Springer-Verlag, Berlin.

(41) Widengren, J. (2001) Photophysical aspects of FCS. In *Fluorescence Correlation Spectroscopy* (Rigler, R., and Elson, E. S., Eds.), pp 276−301, Springer-Verlag, Berlin.

(42) Weber, P. C., Ohlendorf, D. H., Wendolowski, J. J., and Salemme, F. R. (1989) Structural origins of high -affinity biotin binding to streptavidin. *Science 243*, 85−88.

(43) Chevalier, J., Yi, J., Michel, O., and Ming, T. X. (1997) Biotin and digoxigenin as labels for light and electron microscopy in situ hybridization probes: Where do we stand? *J. Histochem. Cytochem. 45*, 481−91.

(44) Gruber, J. H., Kahn, C. D., Kada, G., Riener, C. K., Harms, G. S., Ahrer, W., Dax, T. G., and Knaus, H. (2000) Anomalous fluorescence enhancement of Cy3 and Cy3.5 versus anomalous fluorescence loss of Cy5 and Cy7 upon covalent linking to IgG and noncovalent binding to avidin. *Bioconjugate Chem. 11*, 696−704.

(45) Emans, N., Biwerski, J., and Verkman, A. S. (1995) Imaging of endosome fusion in BHK fibroblasts based on a novel fluorometric avidin−biotin binding assay. *Biophys. J. 69*, 716−728.

(46) Watt, R. M., and Voss, E. W., Jr. (1977) Mechanism of quenching of fluorescein by antifluorescein IgG antibodies. *Immunochemistry 14*, 533−541.

(47) Magde, D., Elson, E. L., and Webb, W. W. (1972) Thermodynamic fluctuations in a reacting system − Measurement by fluorescence correlation spectroscopy. *Phys. Rev. Lett. 29*, 705−708.

(48) Honig, M. G., and Hume, R. I. (1986) Fluorescent carbocyanine dyes allow living neurons of identified origin to be studied in long-term cultures. *J. Cell Biol. 103*, 171−187.

(49) Weston, K. D., and Goldner, L. (2001) Measuring the orientation and reorientation dynamics of single molecules. *J. Phys. Chem. B 105*, 3453−3460.

(50) Bayliss, N. S. (1950) The effect of electrostatic polarization of the solvent on electronic absorption spectra. *J. Chem. Phys. 18*, 292−298.

(51) Rodriguez, J., Scherlis, D., Estrin, D., Aramendia, P. F., and Negri, R. M. (1997) AM1 study of the ground and excited-state potential energy surfaces of symmetric carbocyanines. *J. Phys. Chem. 101*, 6998−7006.

(52) Tinnefeld, P., Buschmann, V., Weston, K. D., and Sauer, M. (2002) Direct Observation of Collective Blinking and Energy Transfer in a Bichromophoric System. *J. Phys. Chem. A*, in press.

BC025600X